Available online at www.sciencedirect.com
ScienceDirect
Journal of Sound and Vibration 322 (2009) 227–240
JOURNAL OF SOUND AND VIBRATION
www.elsevier.com/locate/jsvi

Natural vibration study on rectangular plates with a line hinge and various boundary conditions

M. Huang[a,*], X.Q. Ma[b], T. Sakiyama[a], H. Matsuda[a], C. Morita[a]

[a]*Department of Structural Engineering, Nagasaki University, Nagasaki 852, Japan*
[b]*HeBei University of Technology, PR China*

Received 6 March 2008; received in revised form 2 November 2008; accepted 9 November 2008
Handling Editor: L.G. Tham
Available online 10 January 2009

Abstract

A discrete method is proposed for analyzing the natural vibration problem of rectangular plates with a line hinge. The fundamental differential equations and the solutions of these equations are derived for two parts of the plate, which are obtained by dividing the plate along the line hinge. By transforming these equations into integral equations, and using numerical integration and the continuous conditions along the line hinge, the solutions of the whole plate can be expressed by the unknown quantities on the boundary and the quantities of the rotation along the hinge. The Green function of the deflection problem is used to obtain the characteristic equation of the free vibration. The effects of the position of the line hinge, the aspect ratio, the thickness ratio and the boundary condition on the natural frequency parameters are considered. By comparing the numerical results obtained by the present method with those previously published, the efficiency and accuracy of the present method are investigated.

1. Introduction

The plates with hinge line are often used in engineering as structural elements, such as the boarding platforms of ships, folded gates and chairs. In order to avoid the resonance and ensure the safety of the structures, the study on the vibration problem of these plates is very important. But comparing the free vibration study of plates with complicated cases, such as the plates with point supports [1–4] and the plates with line supports [5–8], the free vibration study of the plates with a line hinge is rather limited. Wang et al. [9] studied the vibration of plates with an internal line hinge by using the Ritz method. The Kirchhoff plate theory was used, so the numerical results were given only for thin plates in which shear stresses were ignored. Xiang and Reddy [10] first provided the exact solutions of natural vibration of rectangular plates by using the Lévy type solution combined with the state-space technique. The abundant solutions were presented. Because the Lévy type solution was used, the exact solutions were only suitable for the plates with two parallel simply supported edges.

*Corresponding author. Tel.: +81 95 8192592.
E-mail address: huang@nagasaki-u.ac.jp (M. Huang).

0022-460X/$ - see front matter © 2008 Elsevier Ltd. All rights reserved.
doi:10.1016/j.jsv.2008.11.006

In this paper, a discrete method [11] is used for analyzing the free vibration of rectangular plates with a line hinge. Thin and moderately thick rectangular plates with various boundary conditions are considered. Basing the first shear deformation theory, the fundamental differential equations of a plate are established for the two parts of the plate obtained by dividing the plate along the hinge. By transforming these equations into integral equations and using numerical integration, the solutions are obtained at the discrete points. Furthermore, by choosing the integral area in an appointed order, the solutions are only related to the unknown quantities on the boundary and the quantities of the rotation along the hinge. That makes the number of unknown quantities decrease greatly. The Green function of the deflection problem is used to obtain the characteristic equation of the free vibration. The efficiency and accuracy of the present method for the rectangular plates with line hinge are investigated by comparing the present results with those reported early. Some new numerical results are given for moderately thick plates with a line hinge and various boundary conditions. The effects of the position of the hinge, the aspect ratio, the thickness ratio and the boundary conditions on the frequency parameters are discussed.

2. Fundamental differential equations

Fig. 1 shows a rectangular plate of length a, width b, density ρ with a line hinge. An xyz coordinate system is used in the present study with its $x-y$ plane contained in the middle plane of the rectangular plate, the z-axis perpendicular to the middle plane of the plate and the origin at one of the corners of the plate. The hinge is parallel to the edges in y-direction and divides the plate into two parts denoted as parts $K = 1$ and 2.

In this paper, the deflection w, the rotations θ_x, θ_y, the shear forces Q_x, Q_y, the twisting moment M_{xy} and the bending moments M_x, M_y are used as variables.

Along the hinge, the plate is divided into two parts. The fundamental differential equations of a part of the plate having a concentrated load $\overline{P}$ at a point (x_q, y_r) are as follows [11]:

$$\frac{\partial Q_x^{(K)}}{\partial x} + \frac{\partial Q_y^{(K)}}{\partial y} + \overline{P}\delta(x - x_q)\delta(y - y_r) = 0, \tag{1a}$$

$$\frac{\partial M_{xy}^{(K)}}{\partial x} + \frac{\partial M_y^{(K)}}{\partial y} - Q_y^{(K)} = 0, \tag{1b}$$

$$\frac{\partial M_x^{(K)}}{\partial x} + \frac{\partial M_{xy}^{(K)}}{\partial y} - Q_x^{(K)} = 0, \tag{1c}$$

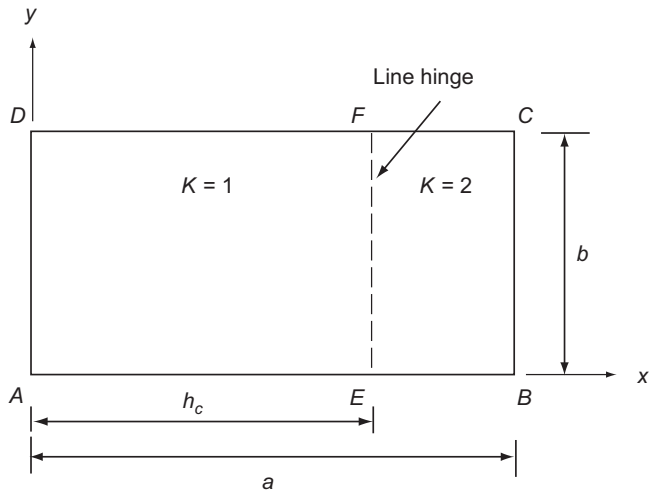

Fig. 1. Rectangular plate with a line hinge.

$$\frac{\partial\theta_x^{(K)}}{\partial x}+v\frac{\partial\theta_y^{(K)}}{\partial y}=\frac{M_x^{(K)}}{D}, \tag{1d}$$

$$\frac{\partial\theta_y^{(K)}}{\partial y}+v\frac{\partial\theta_x^{(K)}}{\partial x}=\frac{M_y^{(K)}}{D}, \tag{1e}$$

$$\frac{\partial\theta_x^{(K)}}{\partial y}+\frac{\partial\theta_y^{(K)}}{\partial x}=\frac{2}{(1-v)}\frac{M_{xy}^{(K)}}{D}, \tag{1f}$$

$$\frac{\partial w^{(K)}}{\partial x}+\theta_x^{(K)}=\frac{Q_x^{(K)}}{Gt_s}, \tag{1g}$$

$$\frac{\partial w^{(K)}}{\partial y}+\theta_y^{(K)}=\frac{Q_y^{(K)}}{Gt_s}, \tag{1h}$$

where the superscript K $(=1,2)$ denotes the Kth part, $D=Eh^3/(12(1-v^2))$ is the bending rigidity; E and G are modulus and shear modulus of elasticity, respectively; v is Poisson's ratio; h is the thickness of plate; $t_s=h/1.2$; $\delta(x-x_q)$ and $\delta(y-y_r)$ are Dirac's delta functions.

By introducing the non-dimensional expressions

$$[X_1^{(K)},X_2^{(K)}]=\frac{a^2}{D_0(1-v^2)}[Q_y^{(K)},Q_x^{(K)}],\quad [X_3^{(K)},X_4^{(K)},X_5^{(K)}]=\frac{a}{D_0(1-v^2)}[M_{xy}^{(K)},M_y^{(K)},M_x^{(K)}],$$

$$[X_6^{(K)},X_7^{(K)},X_8^{(K)}]=[\theta_y^{(K)},\theta_x^{(K)},w^{(K)}/a],$$

Eqs. (1a)–(1h) can also be expressed as the following simple systemized equation:

$$\sum_{s=1}^{8}\left\{F_{1ts}\frac{\partial X_s^{(K)}}{\partial\zeta}+F_{2ts}\frac{\partial X_s^{(K)}}{\partial\eta}+F_{3ts}X_s^{(K)}\right\}+P\delta(\eta-\eta_q)\delta(\zeta-\zeta_r)\delta_{1t}=0\quad(t=1-8), \tag{2}$$

where $\mu=b/a$; $I=\mu(1-v^2)(h_0/h)^3$; $J=2\mu(1+v)(h_0/h)^3$; $T=((1+v)/5)(h_0/a)^2(h_0/h)$; $P=\overline{P}a/(D_0(1-v^2))$; $D_0=Eh_0^3/(12(1-v^2))$ is the standard bending rigidity; h_0 is the standard thickness of the plate; $k=\frac{5}{6}$ is the shear correction factor; $\delta(\eta-\eta_q)$ and $\delta(\zeta-\zeta_r)$ are Dirac's delta functions; δ_{1t} is Kronecker's delta; F_{1ts}, F_{2ts} and F_{3ts} are given in Appendix A.

3. Discrete Green function

As given in Ref. [11], by dividing a rectangular plate vertically into m equal-length divisions and horizontally into n equal-length divisions as shown in Fig. 2, the plate can be considered as a group of discrete points which are the intersections of the $(m+1)$-vertical and $(n+1)$-horizontal dividing lines. To describe the present method conveniently, the rectangular area, $0\leqslant\eta\leqslant\eta_i$, $0\leqslant\zeta\leqslant\zeta_j$, corresponding to the arbitrary intersection (i,j) as shown in Fig. 2 is denoted as the area $[i,j]$, the intersection (i,j) denoted by ◯ is called the main point of the area $[i,j]$, the intersections denoted by ∘ are called the inner dependent points of the area, and the intersections denoted by • are called the boundary dependent points of the area.

By integrating Eq. (2) over the area $[i,j]$ and applying the trapezoidal integration rule, the simultaneous equation for the unknown quantities $X_{sij}^{(K)}=X_s^{(K)}(\eta_i,\zeta_j)$ at the main point (i,j) of the area $[i,j]$ is obtained as follows:

$$\sum_{s=1}^{8}\left\{F_{1ts}\sum_{k=0}^{i}\beta_{ik}(X_{skj}^{(1)}-X_{sk0}^{(1)})+F_{2ts}\sum_{l=0}^{j}\beta_{jl}(X_{sil}^{(1)}-X_{s0l}^{(1)})+F_{3ts}\sum_{k=0}^{i}\sum_{l=0}^{j}\beta_{ik}\beta_{jl}X_{skl}^{(1)}\right\}$$
$$+Pu_{iq}u_{jr}\delta_{1t}=0\quad\text{for the first part,} \tag{3a}$$

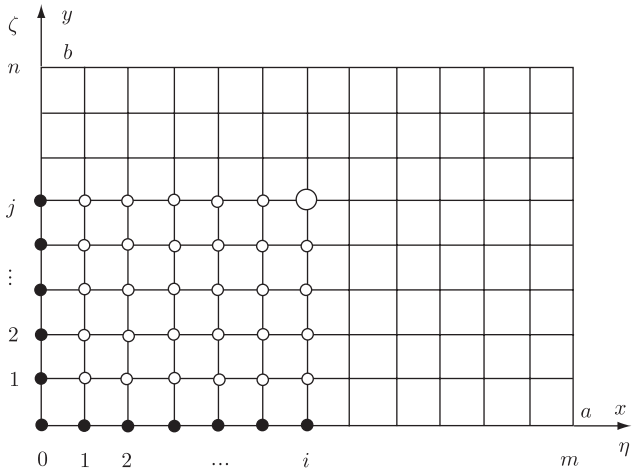

Fig. 2. Discrete points on a rectangular plate.

$$\sum_{s=1}^{8}\left\{F_{1ts}\sum_{k=c}^{i}\beta_{ik}(X_{skj}^{(2)}-X_{sk0}^{(2)})+F_{2ts}\sum_{l=0}^{j}\beta_{jl}(X_{sil}^{(2)}-X_{scl}^{(2)})+F_{3ts}\sum_{k=c}^{i}\sum_{l=0}^{j}\beta_{ik}\beta_{jl}X_{skl}^{(2)}\right\}$$
$$+Pu_{iq}u_{jr}\delta_{1t}=0 \quad \text{for the second part,} \tag{3b}$$

where $t=1-8$, $c=(h_c/a)m$, $\beta_{ik}=\alpha_{ik}/m$; $\beta_{jl}=\alpha_{jl}/n$; $\alpha_{ik}=1-(\delta_{0k}+\delta_{ck}+\delta_{ik})/2$; $\alpha_{jl}=1-(\delta_{0l}+\delta_{jl})/2$; $i=1-m$; $j=1-n$; $u_{iq}=u(\eta_i-\eta_q)$; $u_{jr}=u(\zeta_j-\zeta_r)$.

By retaining the quantities at main point (i,j) on the left-hand side of the equation, putting other quantities on the right-hand side and using the matrix transition, the solution X_{pij} of Eqs. (3a) and (3b) are obtained as follows:

$$X_{pij}^{(1)}=\sum_{t=1}^{8}\left\{\sum_{k=0}^{i}\beta_{ik}A_{pt}[X_{tk0}^{(1)}-X_{tkj}^{(1)}(1-\delta_{ik})]+\sum_{l=0}^{j}\beta_{jl}B_{pt}[X_{t0l}^{(1)}-X_{til}^{(1)}(1-\delta_{jl})]\right.$$
$$\left.+\sum_{k=0}^{i}\sum_{l=0}^{j}\beta_{ik}\beta_{jl}C_{ptkl}X_{tkl}^{(1)}(1-\delta_{ik}\delta_{jl})\right\}-A_{p1}Pu_{iq}u_{jr} \quad \text{for the first part,} \tag{4a}$$

$$X_{pij}^{(2)}=\sum_{t=1}^{8}\left\{\sum_{k=c}^{i}\beta_{ik}A_{pt}[X_{tk0}^{(2)}-X_{tkj}^{(2)}(1-\delta_{ik})]+\sum_{l=0}^{j}\beta_{jl}B_{pt}[X_{tcl}^{(2)}-X_{til}^{(2)}(1-\delta_{jl})]\right.$$
$$\left.+\sum_{k=c}^{i}\sum_{l=0}^{j}\beta_{ik}\beta_{jl}C_{ptkl}X_{tkl}^{(2)}(1-\delta_{ik}\delta_{jl})\right\}-A_{p1}Pu_{iq}u_{jr} \quad \text{for the second part,} \tag{4b}$$

where $p=1-8$, A_{pt}, B_{pt} and C_{ptkl} are given in Appendix A.

In Eq. (4a), the quantity $X_{pij}^{(1)}$ is not only related to the quantities $X_{tk0}^{(1)}$ and $X_{t0l}^{(1)}$ at the boundary dependent points but also the quantities $X_{tkj}^{(1)}$, $X_{til}^{(1)}$ and $X_{tkl}^{(1)}$ at the inner dependent points. In Eq. (4b), the quantity $X_{pij}^{(2)}$ is not only related to the quantity $X_{tk0}^{(2)}$ at the boundary dependent points and the quantity $X_{tcl}^{(2)}$ at the points on the hinged line but also the quantities $X_{tkj}^{(2)}$, $X_{til}^{(2)}$ and $X_{tkl}^{(2)}$ at the inner dependent points. The number of the unknown quantities is rather large. In order to reduce the unknown quantities, the area $[i,j]$ is spread according to the regular order as $[1,1],[1,2],\ldots,[1,n],[2,1],[2,2],\ldots,[2,n],\ldots,[m,1],[m,2],\ldots,[m,n]$. With the spread of the area according to the abovementioned order, the quantities $X_{tkj}^{(K)}$, $X_{til}^{(K)}$ and $X_{tkl}^{(K)}$ at the inner dependent points can be eliminated by substituting the obtained results into the corresponding terms of the right-hand side of Eqs. (4a) and (4b). By repeating this process, the quantity $X_{pij}^{(1)}$ at the main point in the first

part is only related to the quantities $X_{rk0}^{(1)}$ $(r=1,3,4,6,7,8)$ and $X_{s0l}^{(1)}$ $(s=2,3,5,6,7,8)$ at the boundary dependent points. The quantity $X_{pij}^{(2)}$ at the main point in the second part is only related to the quantities $X_{rk0}^{(2)}$ $(r=1,3,4,6,7,8)$ at the boundary dependent points and $X_{scl}^{(2)}$ $(s=2,3,5,6,7,8)$ at points on the hinged line. Therefore, the number of the unknown quantities is reduced greatly. Based on the above consideration, Eqs. (4a) and (4b) are rewritten as follows:

$$X_{pij}^{(1)}=\sum_{d=1}^{6}\left\{\sum_{f=0}^{i}\overline{a}_{pijfd}^{(1)}X_{rf0}^{(1)}+\sum_{g=0}^{j}\overline{b}_{pijgd}^{(1)}X_{s0g}^{(1)}\right\}+\overline{q}_{pij}^{(1)}P \quad \text{for the first part,} \tag{5a}$$

$$X_{pij}^{(2)}=\sum_{d=1}^{6}\left\{\sum_{f=c}^{i}\overline{a}_{pijfd}^{(2)}X_{rf0}^{(2)}+\sum_{g=0}^{j}\overline{b}_{pijgd}^{(2)}X_{scg}^{(2)}\right\}+\overline{q}_{pij}^{(2)}P \quad \text{for the second part,} \tag{5b}$$

where $\overline{a}_{pijfd}^{(K)}$, $\overline{b}_{pijgd}^{(K)}$ and $\overline{q}_{pij}^{(K)}$ $(K=1,2)$ are given in Appendix B.

The boundary conditions at $\eta=0,1,\zeta=0,1$ are

$$X_5=0,\quad X_6=0,\quad X_8=0 \text{ for the simply supported edge at } \eta=0,1, \tag{6a}$$

$$X_6=0,\quad X_7=0,\quad X_8=0 \text{ for the clamped edge at } \eta=0,1, \tag{6b}$$

$$X_2=0,\quad X_3=0,\quad X_5=0 \text{ for the free edge at } \eta=0,1, \tag{6c}$$

$$X_4=0,\quad X_7=0,\quad X_8=0 \text{ for the simply supported edge at } \zeta=0,1, \tag{6d}$$

$$X_6=0,\quad X_7=0,\quad X_8=0 \text{ for the clamped edge at } \zeta=0,1, \tag{6e}$$

$$X_1=0,\quad X_3=0,\quad X_4=0 \text{ for the free edge at } \zeta=0,1. \tag{6f}$$

The continuity conditions at the line hinge are given as

$$X_{2cj}^{(1)}=X_{2cj}^{(2)},\quad X_{3cj}^{(1)}=X_{3cj}^{(2)},\quad X_{5cj}^{(1)}=X_{5cj}^{(2)}=0,\quad X_{6cj}^{(1)}=X_{6cj}^{(2)},\quad X_{8cj}^{(1)}=X_{8cj}^{(2)}. \tag{7}$$

By using the above conditions and the continuity conditions, the unknown quantities in Eqs. (5a) and (5b) can be determined and the discrete solutions can be obtained. The solution of deflection is used as Green function to obtain the characteristic equation of the free vibration.

4. Characteristic equation

By applying the Green function $w(x_0,y_0,x,y)/\overline{P}$ which is the displacement at a point (x_0,y_0) of a plate with a concentrated load $\overline{P}$ at a point (x,y), the displacement amplitude $\hat{w}(x_0,y_0)$ at a point (x_0,y_0) of the rectangular plate with a line hinge during the free vibration is given as follows:

$$\hat{w}(x_0,y_0)=\int_0^a\int_0^b \rho h\omega^2\hat{w}(x,y)[w(x_0,y_0,x,y)/\overline{P}]\,\mathrm{d}x\,\mathrm{d}y, \tag{8}$$

where ρ is the mass density of the plate material.

By using the trapezoidal integration rule and the following non-dimensional expressions:

$$\lambda^4=\frac{\rho_0 h_0\omega^2 a^4}{D_0(1-\nu^2)},\quad k=1/(\mu\lambda^4),\quad H(\eta,\zeta)=\frac{\rho(x,y)}{\rho_0}\frac{h(x,y)}{h_0},$$

$$W(\eta,\zeta)=\frac{\hat{w}(x,y)}{a},\quad G(\eta_0,\zeta_0,\eta,\zeta)=\frac{w(x_0,y_0,x,y)}{a}\frac{D_0(1-\nu^2)}{\overline{P}a},$$

where ρ_0 is the standard mass density, the characteristic equation is obtained from Eq. (8) as

$$\begin{vmatrix} \mathbf{K}_{00} & \mathbf{K}_{01} & \mathbf{K}_{02} & \cdots & \mathbf{K}_{0m} \\ \mathbf{K}_{10} & \mathbf{K}_{11} & \mathbf{K}_{12} & \cdots & \mathbf{K}_{1m} \\ \mathbf{K}_{20} & \mathbf{K}_{21} & \mathbf{K}_{22} & \cdots & \mathbf{K}_{2m} \\ \vdots & \vdots & \vdots & \ddots & \vdots \\ \mathbf{K}_{m0} & \mathbf{K}_{m1} & \mathbf{K}_{m2} & \cdots & \mathbf{K}_{mm} \end{vmatrix} = 0, \tag{9}$$

where

$$\mathbf{K}_{ij} = \beta_{mj} \begin{bmatrix} \beta_{n0}H_{j0}G_{i0j0} - k\delta_{ij} & \beta_{n1}H_{j1}G_{i0j1} & \beta_{n2}H_{j2}G_{i0j2} & \cdots & \beta_{nn}H_{jn}G_{i0jn} \\ \beta_{n0}H_{j0}G_{i1j0} & \beta_{n1}H_{j1}G_{i1j1} - k\delta_{ij} & \beta_{n2}H_{j2}G_{i1j2} & \cdots & \beta_{nn}H_{jn}G_{i1jn} \\ \beta_{n0}H_{j0}G_{i2j0} & \beta_{n1}H_{j1}G_{i2j1} & \beta_{n2}H_{j2}G_{i2j2} - k\delta_{ij} & \cdots & \beta_{nn}H_{jn}G_{i2jn} \\ \vdots & \vdots & \vdots & \ddots & \vdots \\ \beta_{n0}H_{j0}G_{inj0} & \beta_{n1}H_{j1}G_{inj1} & \beta_{n2}H_{j2}G_{inj2} & \cdots & \beta_{nn}H_{jn}G_{injn} - k\delta_{ij} \end{bmatrix}$$

in which $i = 0, 1, \ldots, m; j = 0, 1, \ldots, n$.

From Eq. (9), the natural frequency parameter λ can be obtained by using the QR double-step method and the eigenvectors can be computed by inverse iteration.

5. Numerical results

To investigate the validity of the proposed method, the frequency parameters are given for rectangular plates with a line hinge at $x = h_c$ (shown in Fig. 1). $h_0 = h$ and $\rho_0 = \rho$ are used in the numerical calculation. In all tables and figures, the symbols F, S, and C denote free, simply supported and clamped edges. Four symbols such as CSFS delegate the boundary conditions of the plate, the first indicating the conditions at $x = 0$, the second at $y = 0$, the third at $x = a$ and the fourth at $y = b$. All the convergent values of the frequency parameters are obtained for the plates by using Richardson's extrapolation formula for two cases of divisional numbers m ($= n$). Some of the results are compared with those reported previously.

5.1. Thin rectangular plates with a line hinge

In order to examine the convergency, numerical calculation is carried out by varying the number of divisions m and n for an SSSS square plate with a line hinge at $x = a/2$. The lowest six natural frequency

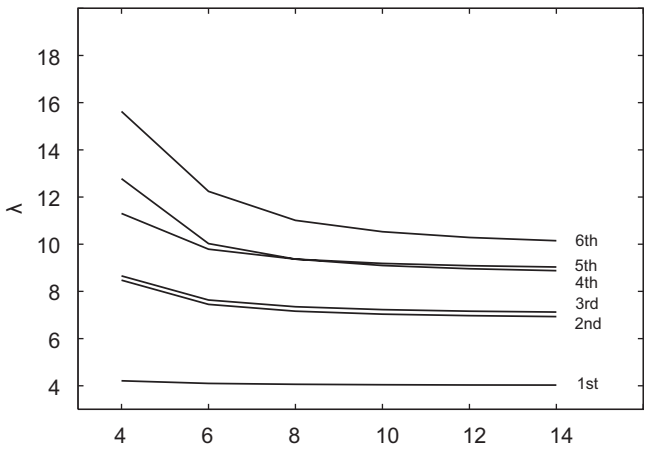

Fig. 3. The natural frequency parameter λ versus the divisional number m ($= n$) for the SSSS square plate with a line hinge at $x = a/2$.

Table 1
Natural frequency parameter λ for SSSS rectangular plates with a line hinge ($h/a = 0.01$).

b/a	h_c/a	References	Mode sequence number					
			1st	2nd	3rd	4th	5th	6th
0.5	1/3	Present	6.864	8.539	11.308	12.837	13.092	13.880
		Ref. [10]	6.869	8.547	11.324	12.852	13.134	13.899
	1/2	Present	6.829	8.879	10.505	12.811	13.952	14.025
		Ref. [10]	6.834	8.884	10.527	12.829	14.043	14.043
1.0	0.1	Present	4.336	6.134	6.992	8.530	8.561	9.894
		Ref. [10]	4.335	6.132	6.994	8.507	8.585	9.909
	0.3	Present	4.092	6.244	6.878	8.470	9.790	9.810
		Ref. [10]	4.093	6.245	6.880	8.473	9.804	9.825
	0.5	Present	4.011	6.826	7.020	8.654	8.876	9.763
		Ref. [10]	4.012	6.829	7.022	8.663	8.879	9.786

parameters of the plate are shown in Fig. 3. It can be found that the numerical results converge monotonously from above with increase in the divisional number and the results of the divisional numbers m $(= n)$ of 12 and 14 are almost same. So it is suitable to obtain the convergent results of frequency parameter by using Richardson's extrapolation formula for two cases of divisional numbers m $(= n)$ of 12 and 14. By repeating the above procedure, the suitable number of divisions m $(= n)$ can be determined for the other plates.

Table 1 shows the numerical values for the lowest six natural frequency parameter λ of SSSS rectangular plates with a line hinge. The cases of $h_c/a = \frac{1}{3}, \frac{1}{2}$ and $0.1, 0.3, 0.5$ are considered for the plates with aspect ratios $b/a = 0.5$ and 1.0, respectively. The exact results obtained by Xiang and Reddy [10] are also shown in the table. It can be seen that the present results agree well with exact results. The mode shapes of the lowest six modes of the above plates are shown in Fig. 4. From Fig. 4, the discontinuity of rotation θ_x can be seen and some changes of mode order for the plate with $b/a = 1.0$ can be found.

Tables 2–4 show the numerical values for the lowest six natural frequency parameter λ of CSCS, CSFS and CSSS rectangular plates with a line hinge and aspect ratio $b/a = 0.5, 1.0$. The cases of $h_c = \frac{1}{3}, \frac{1}{2}, 0.1, 0.3, 0.5$ are considered for CSCS plates. The cases of $h_c = \frac{1}{3}, \frac{1}{2}, \frac{2}{3}, 0.3, 0.5, 0.7$ are considered for CSFS and CSSS plates. These numerical results are in good agreement with those of Xiang and Reddy [10]. The mode shapes of the lowest six modes of CSFS plates are shown in Fig. 5. As shown in Fig. 4, the discontinuity of rotation θ_x and some changes of mode order can be found and the vertical nodal lines will move to the free edge. That shows the vertical nodal lines have the trend to be close to the edge with less boundary constraint.

Table 5 shows the numerical values for the lowest six natural frequency parameter λ of CCCC, CSCC, SSCC and CSFC square plates with a line hinge. The boundary conditions of these plates are not limited to two opposite edges simply supported. The cases of the plates with $h_c/a = 0.1, 0.3, 0.5$ are considered. The results obtained by Wang et al. [9] using Ritz method are also shown in the table. The results of Ref. [9]* are obtained from the table shown in Ref. [9] and those of Ref. [9]** are obtained from the figure in Ref. [9]. But differences between these results for the second frequency parameter are about 5 percent. The present results agree well with those in Ref. [9]**.

5.2. Moderately thick rectangular plates with a line hinge

Table 6 shows the numerical values for the fundamental frequency parameter λ of CSCS with a line hinge and the thickness ratio $h/a = \frac{1}{5}, \frac{1}{7}, \frac{1}{10}, \frac{1}{12}, \frac{1}{15}, \frac{1}{60}, \frac{1}{100}$. Five cases of the position of the line hinge with $h_c/a = 0.1, 0.2, 0.3, 0.4, 0.5$ are considered. From this table, it can be noted that the present results are in good agreement with those of Xiang and Reddy [10] for the plate with variable thickness ratio h/a.

Figs. 6 and 7 show the changes of the fundamental frequency parameter λ with the thickness ratio a/h of CSCS and SSSS plates, respectively. Five cases of the position of the line hinge with $h_c/a = 0.1, 0.2, 0.3, 0.4, 0.5$ are considered. From these figures, it can be found that the fundamental frequency parameter λ increases with

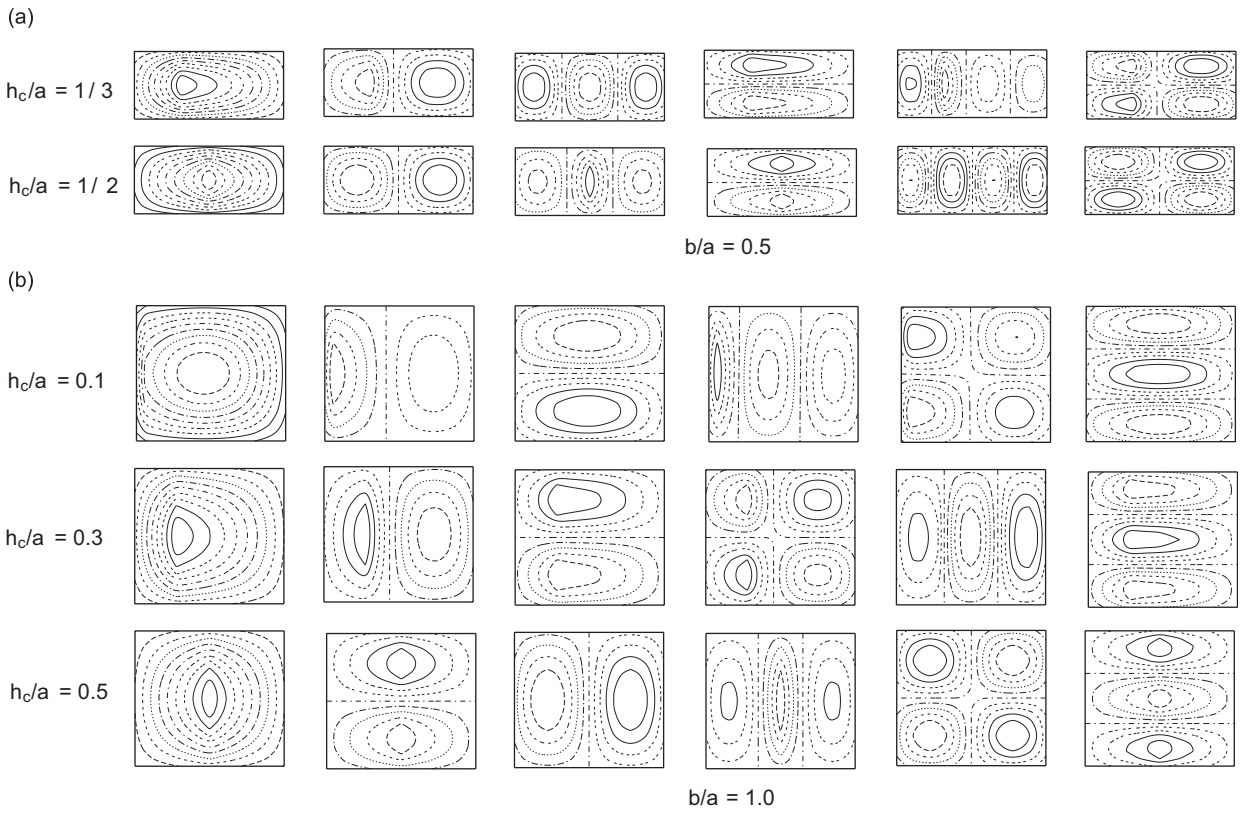

Fig. 4. Mode shapes for SSSS rectangular plates with a line hinge. (a) $b/a = 0.5$; (b) $b/a = 1.0$.

Table 2
Natural frequency parameter λ for CSCS rectangular plates with a line hinge ($h/a = 0.01$).

b/a	h_c/a	References	Mode sequence number					
			1st	2nd	3rd	4th	5th	6th
0.5	1/3	Present	7.209	9.196	12.358	12.923	14.144	14.464
		Ref. [10]	7.215	9.210	12.390	12.942	14.171	14.536
	1/2	Present	7.114	9.711	11.450	12.889	14.348	15.330
		Ref. [10]	7.120	9.723	11.488	12.907	14.369	15.306
1.0	0.1	Present	5.181	7.355	8.255	9.700	10.082	11.301
		Ref. [10]	5.181	7.356	8.260	9.704	10.096	11.328
	0.3	Present	5.167	7.250	7.331	9.131	9.977	10.954
		Ref. [10]	5.167	7.252	7.332	9.135	9.993	10.928
	0.5	Present	4.769	7.111	8.313	9.710	9.906	9.954
		Ref. [10]	4.770	7.114	8.318	9.714	9.923	9.969

increase in the ratio a/h for all the cases. For the plates with the ratio a/h smaller than 20, the increase is obvious. For the plates with the ratio a/h larger than 40, the fundamental frequency parameter λ almost keeps constant. It can also be found that the highest fundamental frequency parameter of the plates with various position of the line hinge can be found at $h_c/a = 0.2$ for CSCS plate and $h_c/a = 0.1$ for SSSS plate. It shows the optimal location of the line hinge changes for the plates with different boundary conditions but does not change for the plates with various thickness ratio.

Table 3
Natural frequency parameter λ for CSFS rectangular plates with a line hinge ($h/a = 0.01$).

b/a	h_c/a	References	Mode sequence number					
			1st	2nd	3rd	4th	5th	6th
0.5	1/3	Present	6.442	7.638	9.705	12.583	12.675	13.246
		Ref. [10]	6.444	7.648	9.719	12.598	12.722	13.269
	1/2	Present	6.412	7.646	10.084	11.795	12.556	13.290
		Ref. [10]	6.416	7.651	10.098	11.842	12.575	13.308
	2/3	Present	6.389	7.868	9.466	12.516	12.534	13.397
		Ref. [10]	6.392	7.875	9.481	12.551	12.560	13.415
1.0	0.3	Present	3.555	5.417	6.444	7.575	7.682	9.565
		Ref. [10]	3.555	5.416	6.446	7.578	7.682	9.496
	0.5	Present	3.540	5.050	6.410	7.644	8.475	9.450
		Ref. [10]	3.540	5.047	6.413	7.642	8.480	9.467
	0.7	Present	3.503	5.446	6.383	7.248	7.904	9.471
		Ref. [10]	3.504	5.484	6.387	7.243	7.903	9.439

Table 4
Natural frequency parameter λ for CSSS rectangular plates with a line hinge ($h/a = 0.01$).

b/a	h_c/a	References	Mode sequence number					
			1st	2nd	3rd	4th	5th	6th
0.5	1/3	Present	7.059	8.774	11.693	12.886	13.978	14.119
		Ref. [10]	7.063	8.785	11.720	12.903	14.002	14.213
	1/2	Present	6.959	9.225	11.040	12.847	14.170	14.424
		Ref. [10]	6.964	9.232	11.069	12.865	14.189	14.521
	2/3	Present	6.975	8.961	11.790	12.868	13.534	14.036
		Ref. [10]	6.980	8.970	11.813	12.885	13.586	14.057
1.0	0.3	Present	4.778	6.734	7.090	8.748	9.905	10.061
		Ref. [10]	4.777	6.735	7.092	8.751	9.920	10.076
	0.5	Present	4.381	6.957	7.509	9.223	9.468	9.833
		Ref. [10]	4.382	6.959	7.511	9.226	9.479	9.847
	0.7	Present	4.334	6.958	7.001	8.849	9.857	10.591
		Ref. [10]	4.343	6.955	6.992	8.863	9.881	10.615

Table 7 shows the numerical values for the lowest six natural frequency parameter λ of moderately thick SSSS, CCCC, CSCS, CSCC and CSFC rectangular plates with a line hinge and aspect ratio $b/a = 0.5, 1$. The cases of $h_c = \frac{1}{3}, \frac{1}{2}, \frac{2}{3}$ are considered for CSFS plates and the cases of $h_c/a = \frac{1}{4}, \frac{1}{3}, \frac{1}{2}$ are considered for the other plates. It can be seen that the boundary conditions, the aspect ratio and the position of the line hinge affect the frequency parameter.

6. Conclusions

A discrete method is used for analyzing the free vibration problem of thin or moderately thick rectangular plate with a line hinge and various boundary conditions. The plate is separated into two parts along the line hinge and the continuous conditions along the hinge are used to obtain the solution of the whole plate. Green function which is the solution of deflection of the bending problem of plate is used to obtain the characteristic equation of the free vibration. The effects of the position of the line hinge, the aspect ratio, the thickness ratio and the boundary condition on the natural frequency parameters of thin or moderately thick rectangular

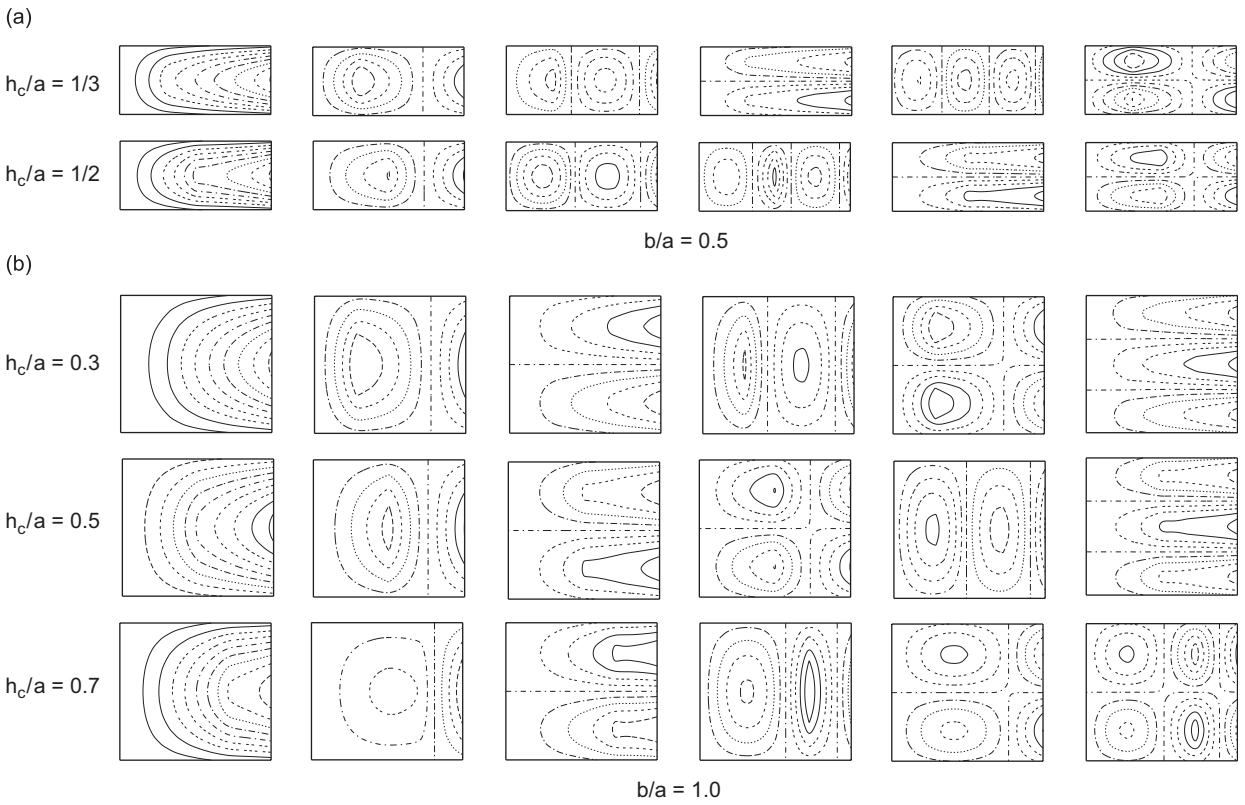

Fig. 5. Mode shapes for CSFS rectangular plates with a line hinge. (a) $b/a = 0.5$; (b) $b/a = 1.0$.

Table 5
Natural frequency parameter λ for square plates with a line hinge and various boundary conditions ($h/a = 0.01$).

BC	h_c/a	References	Mode sequence number					
			1st	2nd	3rd	4th	5th	6th
CCCC	0.1	Present	5.860	8.500	8.531	10.377	11.412	11.437
		Ref. [9]*	5.997	8.069	8.551	–	–	–
		Ref. [9]**	5.9	8.5	8.6	–	–	–
	0.3	Present	5.833	7.669	8.448	9.911	11.088	11.343
		Ref. [9]*	5.643	8.102	8.398	–	–	–
		Ref. [9]**	5.8	7.7	8.5	–	–	–
	0.5	Present	5.566	8.343	8.553	10.148	10.382	11.293
		Ref. [9]*	5.644	7.964	8.432	–	–	–
		Ref. [9]**	5.7	8.4	8.6	–	–	–
CSCC	0.1	Present	5.473	7.921	8.362	10.013	10.746	11.354
	0.3	Present	5.449	7.477	7.826	9.490	10.653	11.016
	0.5	Present	5.143	7.765	8.417	10.022	10.050	10.666
SSCC	0.1	Present	5.043	6.774	7.744	9.270	9.280	10.645
	0.3	Present	4.786	7.119	7.620	9.248	10.560	10.657
	0.5	Present	4.830	7.631	7.660	9.585	9.572	10.597
CSFC	0.1	Present	4.124	5.846	7.173	8.361	8.538	10.317
	0.3	Present	4.180	5.675	7.171	7.704	8.144	9.879
	0.5	Present	4.150	5.321	7.090	7.993	8.544	10.034

Table 6
Fundamental frequency parameter λ for CSCS square plates with a line hinge.

h/a	References	h_c/a				
		0.1	0.2	0.3	0.4	0.5
1/5	Present	4.673	4.769	4.625	4.425	4.351
1/7	Present	4.893	5.006	4.839	4.599	4.512
1/10	Present	5.014	5.175	4.969	4.700	4.607
	Ref. [10]	4.996	–	4.965	–	4.598
1/12	Present	5.125	5.305	5.078	4.786	4.687
1/15	Present	5.168	5.356	5.124	4.823	4.722
1/60	Present	5.177	5.374	5.162	4.866	4.763
1/100	Present	5.181	5.378	5.167	4.872	4.769
	Ref. [10]	5.181	–	5.167	–	4.770

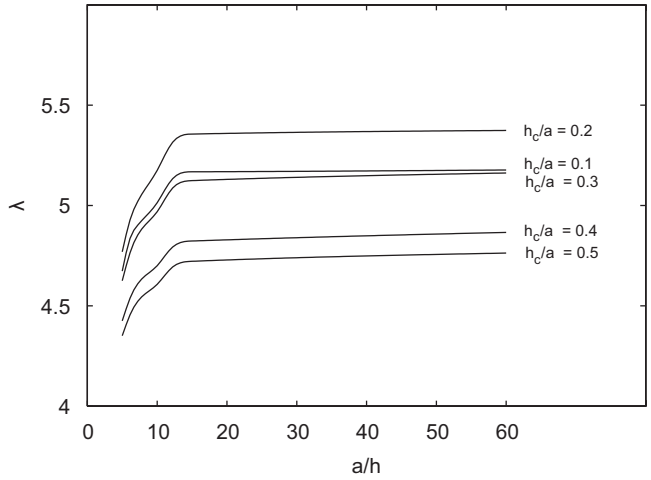

Fig. 6. Fundamental frequency parameters of CSCS square plates versus the thickness ratio a/h for various location of line hinge.

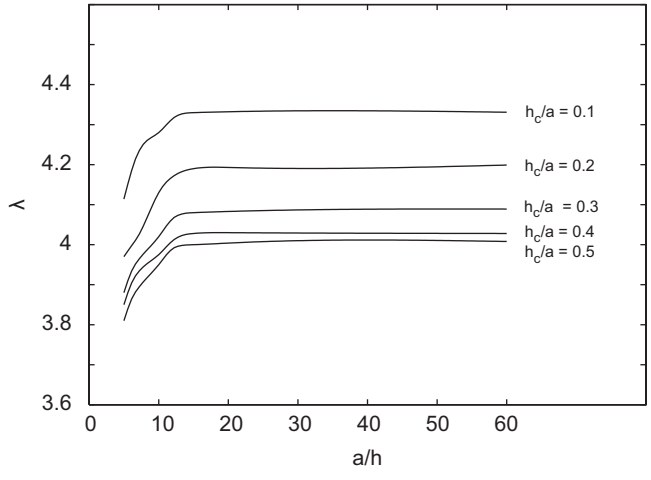

Fig. 7. Fundamental frequency parameters of SSSS square plates versus the thickness ratio a/h for various location of line hinge.

Table 7
Natural frequency parameter λ for rectangular plates with a line hinge ($h/a = 0.2$).

B.C.	b/a	h_c	References	Mode sequence number					
				1st	2nd	3rd	4th	5th	6th
SSSS	0.5	1/4	Present	6.183	7.248	8.866	9.878	10.375	10.429
		1/3	Present	6.149	7.343	9.033	9.865	10.179	10.344
		1/2	Present	6.121	7.565	8.640	9.854	10.436	10.458
	1.0	1/4	Present	3.917	5.576	6.181	7.247	7.954	8.166
		1/3	Present	3.850	5.787	6.119	7.308	8.064	8.137
		1/2	Present	3.808	6.119	6.280	7.546	7.564	8.128
CCCC	0.5	1/4	Present	7.322	8.016	9.251	10.240	10.637	10.678
		1/3	Present	7.286	8.032	9.403	10.230	10.563	10.690
		1/2	Present	7.251	8.220	9.023	10.220	10.637	10.740
	1.0	1/4	Present	5.155	6.442	6.851	7.762	8.326	8.541
		1/3	Present	5.025	6.464	6.801	7.786	8.507	8.572
		1/2	Present	4.879	6.755	6.884	7.950	7.965	8.494
CSCS	0.5	1/4	Present	6.362	7.515	9.053	9.893	10.411	10.554
		1/3	Present	6.293	7.549	9.213	9.877	10.278	10.408
		1/2	Present	6.234	7.779	8.817	9.864	10.491	10.554
	1.0	1/4	Present	4.727	6.294	6.361	7.514	8.213	8.285
		1/3	Present	4.551	6.292	6.321	7.549	8.185	8.525
		1/2	Present	4.351	6.232	6.766	7.779	7.875	8.158
CSCC	0.5	1/4	Present	6.818	7.780	9.147	10.064	10.566	10.594
		1/3	Present	6.898	7.748	9.302	10.103	10.352	10.472
		1/2	Present	6.755	7.995	8.918	10.057	10.596	10.621
	1.0	1/4	Present	4.835	6.402	6.487	7.738	8.292	8.307
		1/3	Present	4.800	6.376	6.600	7.649	8.376	8.548
		1/2	Present	4.529	6.413	6.821	7.886	7.898	8.227
CSFC	0.5	1/3	Present	6.590	6.967	8.164	9.642	10.015	10.234
		1/2	Present	6.343	6.876	8.188	9.367	9.877	10.167
		2/3	Present	6.202	6.959	7.852	9.485	9.803	10.178
	1.0	1/3	Present	3.864	4.927	6.157	6.774	6.848	8.106
		1/2	Present	3.819	4.720	6.097	6.754	7.059	8.125
		2/3	Present	3.743	4.875	6.050	6.331	6.785	7.836

plates are considered. By comparing the numerical results obtained by the present method with those previously published, the efficiency and accuracy of the present method are investigated.

Appendix A

$F_{111} = F_{124} = F_{133} = F_{156} = F_{167} = F_{188} = 1$, $F_{146} = v$, $F_{212} = F_{223} = F_{235} = F_{247} = F_{266} = \mu$, $F_{257} = \mu v$, $F_{278} = 1$, $F_{321} = F_{332} = -\mu$, $F_{345} = F_{354} = -I$, $F_{363} = -J$, $F_{372} = -T$, $F_{377} = 1$, $F_{381} = -\mu T$, $F_{386} = \mu$, other $F_{kts} = 0$.

$A_{p1} = \gamma_{p1}$, $A_{p2} = 0$, $A_{p3} = \gamma_{p2}$, $A_{p4} = \gamma_{p3}$, $A_{p5} = 0$, $A_{p6} = \gamma_{p4} + v\gamma_{p5}$, $A_{p7} = \gamma_{p6}$, $A_{p8} = \gamma_{p7}$.

$B_{p1} = 0$, $B_{p2} = \mu\gamma_{p1}$, $B_{p3} = \mu\gamma_{p3}$, $B_{p4} = 0$, $B_{p5} = \mu\gamma_{p2}$, $B_{p6} = \mu\gamma_{p6}$, $B_{p7} = \mu(v\gamma_{p1} + \gamma_{p5})$, $B_{p8} = \gamma_{p8}$.

$C_{p1kl} = \mu(\gamma_{p3} + k_{kl}\gamma_{p7})$, $C_{p2kl} = \mu\gamma_{p2} + k_{kl}\gamma_{p8}$, $C_{p3kl} = J\gamma_{p6}$, $C_{p4kl} = I_{kl}\gamma_{p4}$, $C_{p5kl} = I_{kl}\gamma_{p5}$, $C_{p6kl} = -\mu\gamma_{p7}$, $C_{p7kl} = -\gamma_{p8}$, $C_{p8kl} = 0$.

$[\gamma_{pk}] = [\overline{\gamma}_{pk}]^{-1}$, $\overline{\gamma}_{11} = \beta_{ii}$, $\overline{\gamma}_{12} = \mu\beta_{jj}$, $\overline{\gamma}_{22} = -\mu\beta_{ij}$, $\overline{\gamma}_{23} = \beta_{ii}$, $\overline{\gamma}_{25} = \mu\beta_{jj}$, $\overline{\gamma}_{31} = -\mu\beta_{ij}$, $\overline{\gamma}_{33} = \mu\beta_{jj}$, $\overline{\gamma}_{34} = \beta_{ii}$, $\overline{\gamma}_{44} = -I_{ij}\beta_{ij}$, $\overline{\gamma}_{46} = \beta_{ii}$,$\overline{\gamma}_{47} = \mu v\beta_{jj}$, $\overline{\gamma}_{55} = -I_{ij}\beta_{ij}$, $\overline{\gamma}_{56} = v\beta_{ii}$, $\overline{\gamma}_{57} = \mu\beta_{jj}$, $\overline{\gamma}_{63} = -J_{ij}\beta_{ii}$, $\overline{\gamma}_{66} = \mu\beta_{jj}$, $\overline{\gamma}_{67} = \beta_{ii}$, $\overline{\gamma}_{71} = -\mu k_{ij}\beta_{ij}$, $\overline{\gamma}_{76} = \mu\beta_{ij}$, $\overline{\gamma}_{78} = \beta_{ii}$, $\overline{\gamma}_{82} = -H_{ij}\beta_{ij}$,$\overline{\gamma}_{87} = \beta_{ij}$, $\overline{\gamma}_{88} = \beta_{jj}$, other $\overline{\gamma}_{pk} = 0$, $\beta_{ij} = \beta_{ii}\beta_{jj}$.

Appendix B

$\overline{a}^{(1)}_{1i0i1}=\overline{a}^{(1)}_{3i0i2}=\overline{a}^{(1)}_{4i0i3}=\overline{a}^{(1)}_{6i0i4}=\overline{a}^{(1)}_{7i0i5}=\overline{a}^{(1)}_{8i0i6}=1,\qquad \overline{b}^{(1)}_{20jj1}=\overline{b}^{(1)}_{30jj2}=\overline{b}^{(1)}_{50jj3}=\overline{b}^{(1)}_{60jj4}=\overline{b}^{(1)}_{70jj5}=\overline{b}^{(1)}_{80jj6}=1,$
$\overline{b}^{(1)}_{30002}=0.$

$\overline{a}^{(2)}_{1i0i1}=\overline{a}^{(2)}_{3i0i2}=\overline{a}^{(2)}_{4i0i3}=\overline{a}^{(2)}_{6i0i4}=\overline{a}^{(2)}_{7i0i5}=\overline{a}^{(2)}_{8i0i6}=1,\qquad \overline{b}^{(2)}_{2cjj1}=\overline{b}^{(2)}_{3cjj2}=\overline{b}^{(2)}_{5cjj3}=\overline{b}^{(2)}_{6cjj4}=\overline{b}^{(2)}_{7cjj5}=\overline{b}^{(2)}_{8cjj6}=1,$
$\overline{b}^{(2)}_{3c0c2}=0.$

$$\overline{a}^{(1)}_{pijfd}=\sum_{t=1}^{8}\left\{\sum_{k=0}^{i}\beta_{ik}A_{pt}[\overline{a}^{(1)}_{tk0fd}-\overline{a}^{(1)}_{tkjfd}(1-\delta_{ki})]+\sum_{l=0}^{j}\beta_{jl}B_{pt}[\overline{a}^{(1)}_{t0lfd}-\overline{a}^{(1)}_{tilfd}(1-\delta_{lj})]+\sum_{k=0}^{i}\sum_{l=0}^{j}\beta_{ik}\beta_{jl}C_{ptkl}\overline{a}^{(1)}_{tklfd}(1-\delta_{ki}\delta_{lj})\right\},$$

$$\overline{b}^{(1)}_{pijgd}=\sum_{t=1}^{8}\left\{\sum_{k=0}^{i}\beta_{ik}A_{pt}[\overline{b}^{(1)}_{tk0gd}-\overline{b}^{(1)}_{tkjgd}(1-\delta_{ki})]+\sum_{l=0}^{j}\beta_{jl}B_{pt}[\overline{b}^{(1)}_{t0lgd}-\overline{b}^{(1)}_{tilgd}(1-\delta_{lj})]+\sum_{k=0}^{i}\sum_{l=0}^{j}\beta_{ik}\beta_{jl}C_{ptkl}\overline{b}^{(1)}_{tklgd}(1-\delta_{ki}\delta_{lj})\right\},$$

$$\overline{q}^{(1)}_{pij}=\sum_{t=1}^{8}\left\{\sum_{k=0}^{i}\beta_{ik}A_{pt}[\overline{q}^{(1)}_{tk0}-\overline{q}^{(1)}_{tkj}(1-\delta_{ki})]+\sum_{l=0}^{j}\beta_{jl}B_{pt}[\overline{q}^{(1)}_{t0l}-\overline{q}^{(1)}_{til}(1-\delta_{lj})]+\sum_{k=0}^{i}\sum_{l=0}^{j}\beta_{ik}\beta_{jl}C_{ptkl}\overline{q}^{(1)}_{tkl}(1-\delta_{ki}\delta_{lj})\right\}-A_{p1}u_{iq}u_{jr},$$

$$\overline{a}^{(2)}_{pijfd}=\sum_{t=1}^{8}\left\{\sum_{k=c}^{i}\beta_{ik}A_{pt}[\overline{a}^{(2)}_{tk0fd}-\overline{a}^{(2)}_{tkjfd}(1-\delta_{ki})]+\sum_{l=0}^{j}\beta_{jl}B_{pt}[\overline{a}^{(2)}_{tclfd}-\overline{a}^{(2)}_{tilfd}(1-\delta_{lj})]+\sum_{k=c}^{i}\sum_{l=0}^{j}\beta_{ik}\beta_{jl}C_{ptkl}\overline{a}^{(2)}_{tklfd}(1-\delta_{ki}\delta_{lj})\right\},$$

$$\overline{b}^{(2)}_{pijgd}=\sum_{t=1}^{8}\left\{\sum_{k=c}^{i}\beta_{ik}A_{pt}[\overline{b}^{(2)}_{tk0gd}-\overline{b}^{(2)}_{tkjgd}(1-\delta_{ki})]+\sum_{l=0}^{j}\beta_{jl}B_{pt}[\overline{b}^{(2)}_{tclgd}-\overline{b}^{(2)}_{tilgd}(1-\delta_{lj})]+\sum_{k=c}^{i}\sum_{l=0}^{j}\beta_{ik}\beta_{jl}C_{ptkl}\overline{b}^{(2)}_{tklgd}(1-\delta_{ki}\delta_{lj})\right\},$$

$$\overline{q}^{(2)}_{pij}=\sum_{t=1}^{8}\left\{\sum_{k=c}^{i}\beta_{ik}A_{pt}[\overline{q}^{(2)}_{tk0}-\overline{q}^{(2)}_{tkj}(1-\delta_{ki})]+\sum_{l=0}^{j}\beta_{jl}B_{pt}[\overline{q}^{(2)}_{tcl}-\overline{q}^{(2)}_{til}(1-\delta_{lj})]+\sum_{k=c}^{i}\sum_{l=0}^{j}\beta_{ik}\beta_{jl}C_{ptkl}\overline{q}^{(2)}_{tkl}(1-\delta_{ki}\delta_{lj})\right\}-A_{p1}u_{iq}u_{jr}.$$

References

[1] H.T. Saliba, Free vibration analysis of rectangular cantilever plates with symmetrically distributed lateral point supports, *Journal of Sound and Vibration* 127 (1988) 77–89.

[2] A.V. Bapat, N. Venkatramani, S. Suryanarayan, The use of flexibility functions with negative domains in the vibration analysis of asymmetrically point-supported rectangular plates, *Journal of Sound and Vibration* 124 (1988) 555–576.
[3] A.V. Bapat, S. Suryanarayan, Free vibrations of rectangular plates with interior point supports, *Journal of Sound and Vibration* 134 (1989) 291–313.
[4] M. Huang, X.Q. Ma, T. Sakiyama, H. Matsuda, C. Morita, Free vibration analysis of rectangular plates with variable thickness and point supports, *Journal of Sound and Vibration* 300 (2007) 435–452.
[5] M.-H. Huang, D.P. Thambiratnam, Free vibration analysis of rectangular plates on elastic intermediate supports, *Journal of Engineering Mechanics* 240 (2001) 567–580.
[6] K. Takahashi, T. Chishaki, Free vibrations of two-way continuous rectangular plates, *Journal of Sound and Vibration* 62 (1979) 455–459.
[7] D.J. Gorman, Solutions of the Ĺevy type for the free vibration analysis of diagonally supported rectangular plates, *Journal of Sound and Vibration* 66 (1979) 239–246.
[8] S. Azimi, J.F. Hamilton, W. Soedel, The receptance method applied to the free vibration of continuous rectangular plates, *Journal of Sound and Vibration* 93 (1984) 9–29.
[9] C.M. Wang, Y. Xiang, C.Y. Wang, Buckling and vibration of plates with an internal line-hinge via the Ritz method, in: *Proceedings of First Asian-Pacific Congress on Computational Mechanics*, Sydney, 2001, pp. 163–1672.
[10] Y. Xiang, J.N. Reddy, Natural vibration of rectangular plates with an internal line hinge using the first order shear deformation plate theory, *Journal of Sound and Vibration* 263 (2003) 285–297.
[11] M. Huang, X.Q. Ma, T. Sakiyama, H. Matsuda, C. Morita, Free vibration analysis of orthotropic rectangular plates with variable thickness and general boundary conditions, *Journal of Sound and Vibration* 288 (2005) 931–955.